Electronic Supplementary Information for

Binaphthyl-based chiral covalent organic frameworks for chiral drugs separation

Hui-Chao Ma,*‡ Hai-Ping Jiang,‡ Zi-Hui Yao, Jun-Feng Tan, Yang-Yang Xing, Gong-Jun Chen*

and Yu-Bin Dong*

College of Chemistry, Chemical Engineering and Materials Science, Collaborative Innovation Center of

Functionalized Probes for Chemical Imaging in Universities of Shandong, Key Laboratory of Molecular and

Nano Probes, Ministry of Education, Shandong Normal University, Jinan 250014, P. R. China.

Email: huichaoma@sdnu.edu.cn, gongjchen@126.com, yubindong@sdnu.edu.cn

Contents

1. Materials and instruments

The reagents and solvents are commercially available and used without further purification. Building block 2, 4, 6-triformylphloroglucinol (TP) was synthesized according to previously published procedure. (*R*)- and (*S*)-DCDB were synthesized according to our reported procedure. [1]

The powder diffractometer (XRD) patterns were collected by a D8 ADVANCEX-ray with Cu Kα radiation (λ = 1.5405 Å). The total surface areas of the catalysts were measured by the BET (Brunauer–Emmer–Teller) method using N_2 adsorption at 77 K, this was done by the Micromeritics ASAP 2000 sorption/desorption analyzer. HRTEM (High resolution transmission electron microscopy) analysis was performed on a JEOL 2100 Electron Microscope at an operating voltage of 200 kV. Scanning electron microscopy (SEM) images were taken on a SUB010 scanning electron microscope with acceleration voltage of 20 kV. Elemental analyses for C, H and N were obtained on a Perkin-Elmer analyzer model 240. Infrared (IR) samples were prepared as KBr pellets, and spectra were obtained in the 400-4000 cm^{-1} range using a Perkin-Elmer 1600 FTIR spectrometer. ^{13}C solid-state NMR spectra were recorded on a MERCURY plus 400 spectrometer operating at resonance frequencies of 400 MHz. Thermogravimetric analyses (TGA) were carried out under flowing nitrogen at a heating rate of 10 °C·min^{-1} on a TA Instrument Q5 analyzer. High-resolution mass spectrometry (HRMS) analysis was carried out on a Bruker maXis ultrahigh-resolution-TOF mass spectrometer. The solid-state CD spectra were recorded on a J-815 spectropolarimeter (Jasco, Japan). ^1H NMR data were collected on an AM-400 spectrometer. Chemical shiftsare reported in δ relative to TMS. Enantiomer ratios were determined by chiral HPLC analysis using a Shimadzu LC-10AT VP series and a Shimadzu LC-10A VP UV-vis.

2. Synthesis of monomers

(*R*)-DCDB   (*R*)-BINOLDE   (*R*)-BINOLDH
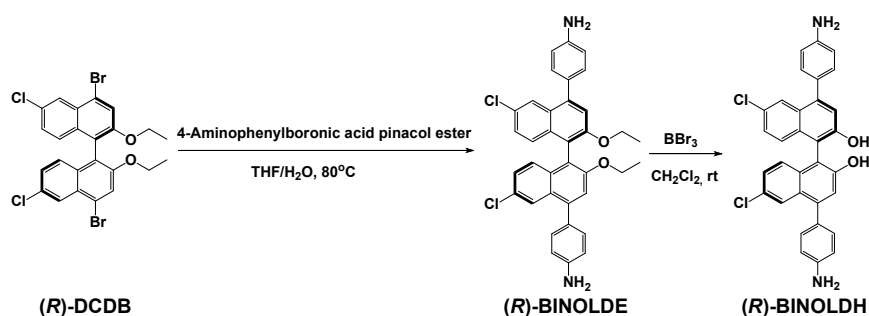
Under nitrogen, a mixture of (*R*)-DCDB (0.57g, 1.0 mmol), 4-aminophenylboronic acid pinacol ester (0.44 g, 2.0 mmol), Pd(PPh$_3$)$_4$ (0.08 g, 0.06 mmol) and K$_2$CO$_3$ (0.82 g, 6.0 mmol) in THF (30 mL)/H$_2$O (10.0 mL) was refluxed for 36 h. After removed the solvent, the residue was redissolved in CH$_2$Cl$_2$ and dried over MgSO$_4$. The obtained crude product was purified by the column on silica gel using CH$_2$Cl$_2$/THF (10:1, v/v) as eluent to give (*R*)-BINOLDE in 83% yield. ^{1}H NMR (400 MHz, CDCl$_3$) δ=7.88 (d, J = 7.1 Hz, 1H), 7.70 (t, J = 25.5 Hz, 1H), 7.34 (d, J = 16.0 Hz, 1H), 7.26-7.12 (m, 1H), 4.11 (d, J = 6.7 Hz, 1H), 1.13 (t, J = 6.1 Hz, 1H). IR (KBr pellet cm^{-1}): 3203(vs), 2262(w), 1494(s), 1366(m), 1175(s), 1145(m), 1040(w), 946(m), 884(w), 826(w), 726(m), 637(w), 549(m). ^{13}C NMR (400 MHz, CDCl$_3$): δ 156.13, 144.54, 136.76, 132.97, 132.05, 129.06, 128.24, 127.75, 126.28, 122.85, 120.63, 119.97, 118.94, 62.7, 15.2. ESI-MS: m/z, Anal. Calcd: 615.14, Exp: 615.14, [M+Na]$^+$.

(*R*)-BINOLDH was obtained by stirring the suspended (*R*)-BINOLDE (0.61 g, 1.0 mmol) in CH$_2$Cl$_2$ (10.0mL) with excess BBr$_3$ (570 µL, 6.0 mmol) for 24 h. Quenching reaction with ice water, the organic layer was separated, and the aqueous layer was completely extracted with CH$_2$Cl$_2$, dried with MgSO$_4$ and concentrated in vacuo to provide (*R*)-BINOLDH (86%) as a beige crystalline solid. ^{1}H NMR (400 MHz, DMSO): δ=7.48-7.22 (m, 4H), 7.05 (dd, J = 42.9, 27.0 Hz, 1H), 0.00 (d, J = 63.5 Hz, 2H), 0.00 (dd, J = 44.3, 13.7 Hz, 3H), 0.00 (d, J = 43.5 Hz, 1H). IR (KBr pellet cm-1): 3203(vs), 2262(w), 1586(w), 1490(s), 1377(m), 1195(s), 1149(w), 1020(w), 946(w), 884(w), 816(w), 726(m), 636(m), 549(m). ^{13}C NMR (400 MHz, CDCl$_3$): δ 155.21, 146.84, 144.34, 137.62, 132.75, 131.26, 128.07, 127.04, 126.76, 124.31, 119.86, 118.73, 115.60.

ESI-MS: m/z, Anal. Calcd: 537.10, Exp: 537.11, [M+Na]$^+$. (*S*)-BINOLDH was synthesized following the same method mentioned above except that (*S*)-DCDB was used instead of (*R*)-DCDB.

3. Synthesis of (*R*)- and (*S*)-BHTP-COF

An *o*-dichlorobenzene (*o*-DCB)/*n*-BuOH (0.5/0.5 mL) mixture of (*R*)- or (*S*)-BINOLDH (0.12 mmol, 64.5 mg), TP (0.08 mmol, 16.8 mg) and acetic acid (30 µL) in a Pyrex tube (35 mL) were degassed via three freeze-pump-thaw cycles. The tube was sealed and heated under N$_2$ at 120 °C in an oil bath for 3 days. The solids were separated via centrifugation after cooling to room temperature. The powder was washed several

times with dichloromethane and ethanol via centrifugation and dried under vacuum to produce (*R*)- or (*S*)-

BHTP-COF in 92 % yield. Elemental Analysis (%) calcd for $C_{14}H_{11}N_2O$: C, 75.32; N, 12.55; H, 4.97. Found (%):

C, 76.15; N, 12.13; H, 5.31.

4. General procedure for column packing

The stationary material materials including (*R*)- or (*S*)-**BHTP-COF** materials were packed with the same

method. (*R*)- or (*S*)-**BHTP-COF** was dispersed in a mixture of *n*-hexane/isopropanol (9:1, v/v) for 10 min.

The suspension was then packed into an empty stainless-steel column (20 cm long x 4.2 mm id) under 40

MPa using *n*-hexane/isopropanol as the displacement liquid. The prepared columns were conditioned with

n-hexane/isopropanol (9:1, v/v) at a flow rate of 0.5 mL/min for 2 h before chromatographic experiments.

Separation factor (*α*) and resolution factor (*Rs*) were obtained from the following equations:

$$\alpha = (t_{R2} - t_0)/(t_{R1} - t_0) \qquad Rs = 2(t_{R2} - t_{R1})/(w_1 + w_2)$$

Where t_{R1} and t_{R2} represent the retention times of right-handed or left-handed enantiomers ($t_{R2} > t_{R1}$),

and w_1 and w_2 are the widths of the bases formed by triangulation of the peaks, respectively. The column

void time is t_0.

5. Figures S1-S5

c

d

e
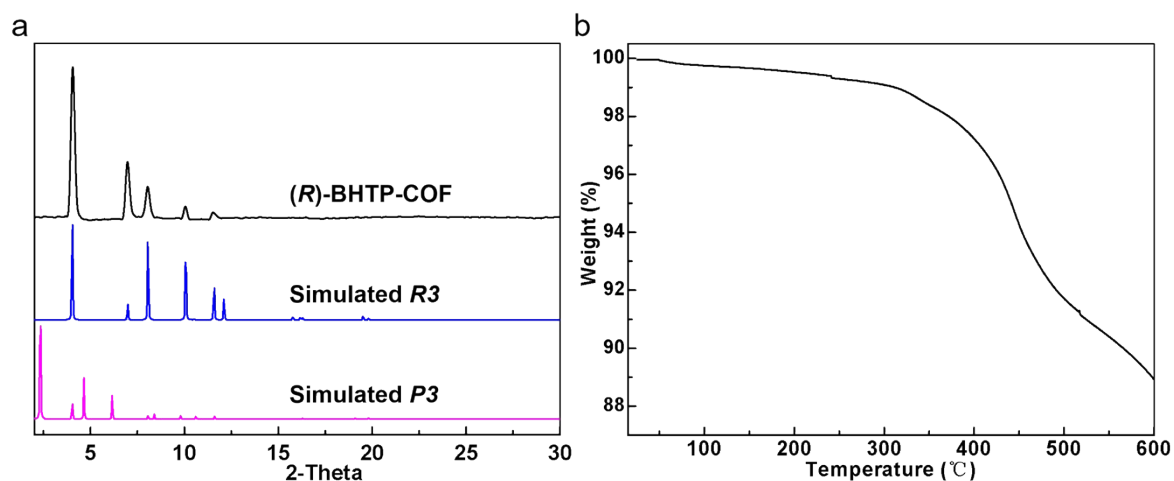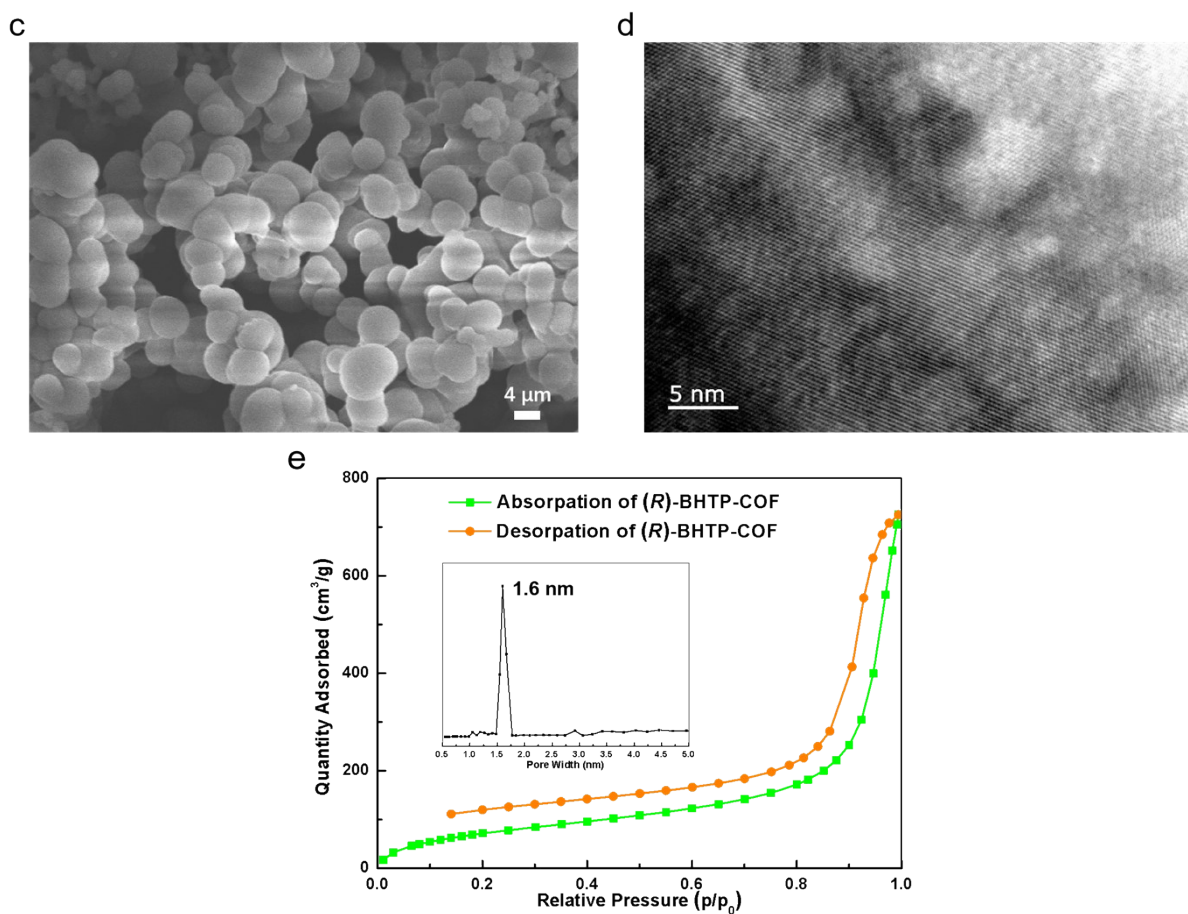
Fig. S1 Characterization of (*R*)-**BHTP-COF**. (a) Measured and simulated PXRD patterns for (*R*)-**BHTP-COF**. Compared to the pattern generated from the *P3* space group (pink line), (*R*)-**BHTP-COF** unequivocally crystallizes in the *R3* space group (blue line). (b) TGA trace of (*R*)-**BHTP-COF**. (c) SEM image of (*R*)-**BHTP-COF**. (d) HR-TEM image of (*R*)-**BHTP-COF**. (e) N_2 adsorption and desorption isotherms of (*R*)-**BHTP-COF** at 77 K. Its pore width distribution is inserted.

a

b

c

d

e

f

(*S*)-BHTP-COF

Simulated *R3*

Simulated *P3*

g

h
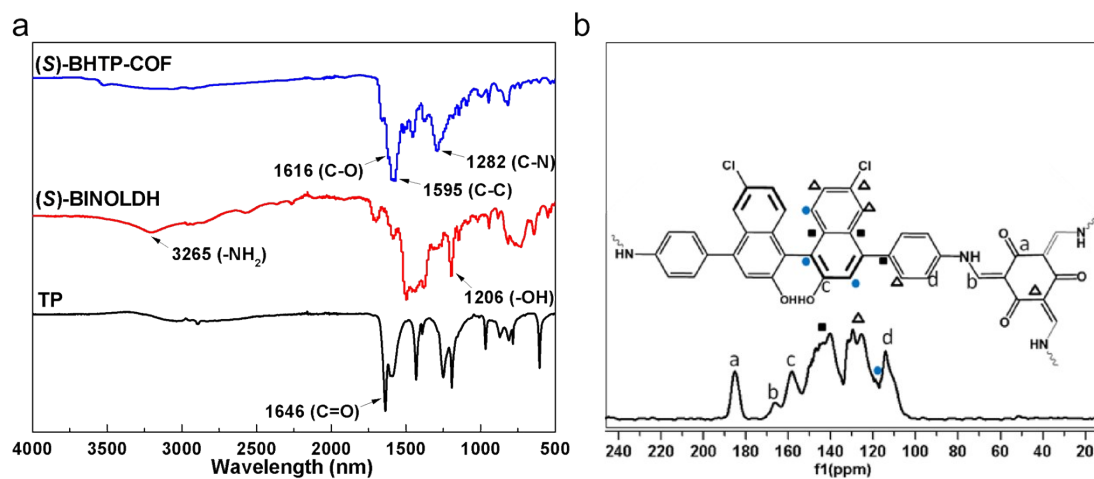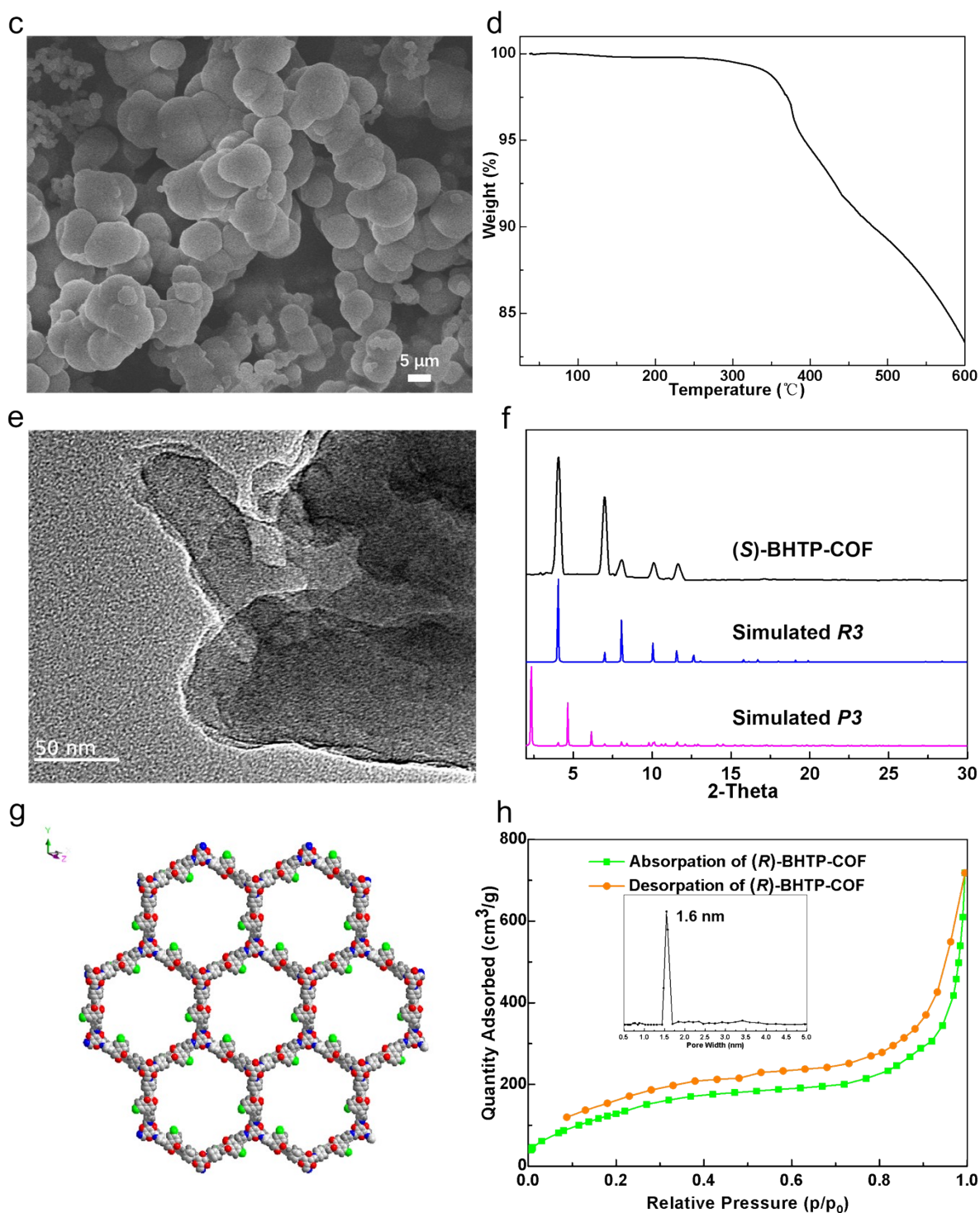
Fig. S2 Characterization of (*S*)-**BHTP-COF**. (a) FT-IR spectra of (*S*)-**BHTP-COF** and its monomers. (b) Solid-

state ¹³C CP-MAS NMR spectrum of (*S*)-**BHTP-COF**. (c) SEM image of (*S*)-**BHTP-COF**. (d) TGA trace of (*S*)-

BHTP-COF. (e) SEM image of (*S*)-**BHTP-COF**. (f) Measured and simulated PXRD patterns for (*S*)-**BHTP-COF**.

Compared to the pattern generated from the *P3* space group (pink line), (*S*)-**BHTP-COF** unequivocally

crystallizes in the *R3* space group (blue line). (g) Crystal structure of (*S*)-**BHTP-COF**. (h) N_2 adsorption and desorption isotherms of (*S*)-**BHTP-COF** at 77 K. Its pore width distribution is inserted.
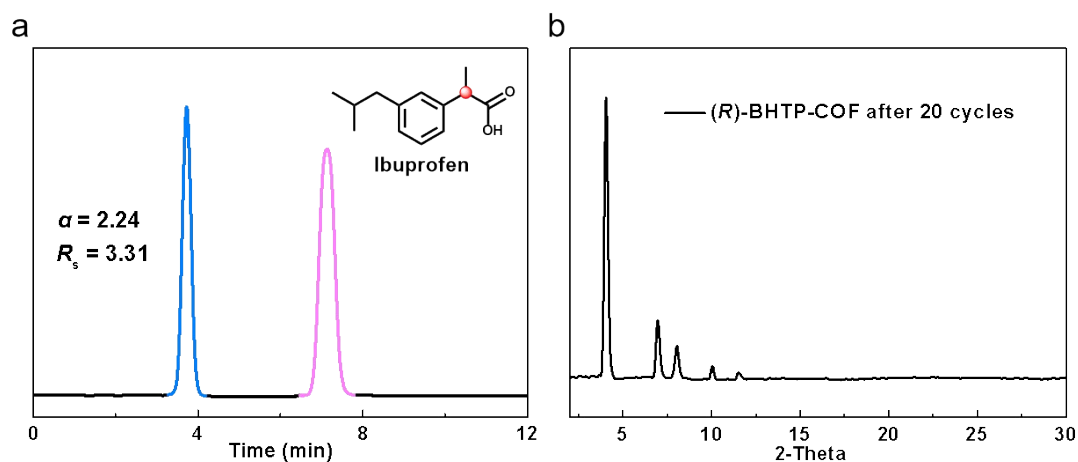
Fig. S3 (a) HPLC romatograms of ibuprofen enantiomers on the (*R*)-**BHTP-COF** packed column using the same eluent conditions obtained for 20 inject runs. (b) PXRD pattern of the (*R*)-**BHTP-COF** after 20 catalytic cycles.
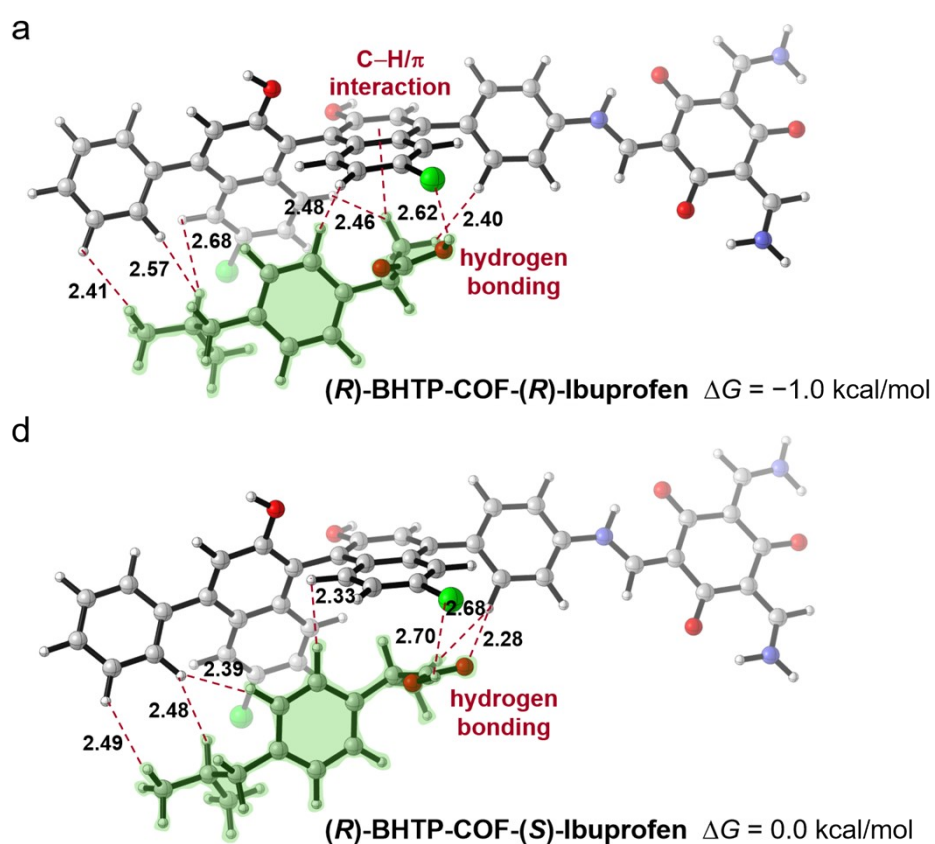
Fig. S4 The molecular models of the ibuprofen *R*-enantiomer (a) and *S*-enantiomer (b) interacting with (*R*)-

BHTP-COF (The bond distances given in angstroms). All density functional theory (DFT) calculations were performed with the Gaussian16 package. [2] The geometry optimizations were carried out in the gas phase at the B3LYP level of theory [3,4] with additional Grimme's D3 dispersion correction (Becke-Johnson damping), [5] with the def2-SVP basis set. [6,7] The 3D structures shown were illustrated using CYLview. [8]
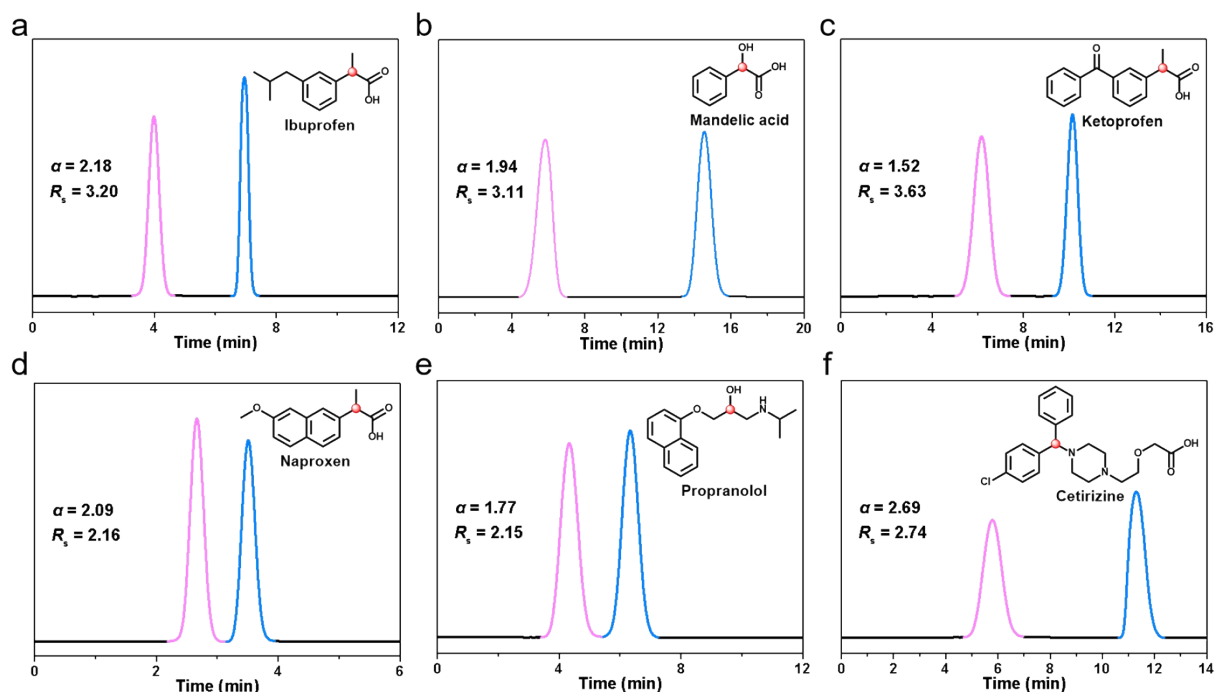

Fig. S5 HPLC chromatograms of the six racemic drugs including ibuprofen(a), mandelic acid (b), ketoprofen(c), naproxen(d), propranolol (e), cetirizine (f) with the (*S*)-**BHTP-COF** packed column (mobile phase n-hexane/isopropanol (9:1, v/v), 0.3 mL/min flow rate, detection wavelength 254 nm, temperature 25 °C).

6. Tables S1-S4

Table S1. The structure model of (*R*)-**BHTP-COF** with *R3* mode.

(*R*)-**BHTP-COF** Space group: *R3* $a = 43.8379$ Å, $b = 43.8379$ Å, $c = 9.0257$ Å $\alpha = 90.0°$, $\beta = 90°$, $\gamma = 120.0°$			
Atom	x	y	z
C1	-1.30833	0.32246	0.34009
C2	-1.29726	-0.64152	0.33956
C3	-1.20655	-0.59797	0.20363
C4	-1.1937	-0.56897	0.10834

C5	-1.15759	-0.54413	0.10086
C6	-1.13392	-0.55002	0.18775
C7	-1.14714	-0.57748	0.29382
C8	-1.18337	-0.60149	0.29864
C9	-1.09529	-0.53323	0.17966
C10	-1.07522	-0.5154	0.05329
C11	-1.03794	-0.49977	0.05801
C12	-1.02154	-0.50303	0.18771
C13	-1.04175	-0.52156	0.31149
C14	-1.07841	-0.53602	0.30652
C15	-0.98283	-0.48787	0.19704
C16	-0.96305	-0.45593	0.27364
C17	-0.92655	-0.44196	0.29005
C18	-0.90967	-0.45931	0.23254
C19	-0.9298	-0.49253	0.16222
C20	-0.96655	-0.50644	0.14144
C21	-0.84913	-0.44516	0.34037
C22	-0.87084	-0.44019	0.23735
C23	-0.85548	-0.41581	0.11924
C24	-0.81877	-0.3946	0.11358
C25	-0.79732	-0.39822	0.218
C26	-0.81242	-0.42372	0.32881
C27	-0.70329	-0.35581	0.09487
C28	-0.68907	-0.31924	0.0948
C29	-1.09126	-0.51211	-0.07669
C30	-1.07098	-0.49388	-0.19955
C31	-1.03444	-0.47855	-0.19473
C32	-1.01798	-0.48135	-0.06739
C33	-0.98635	-0.53899	0.06744
C34	-0.97039	-0.55771	0.0173
C35	-0.93469	-0.54485	0.04266
C36	-0.91461	-0.51281	0.11582
O37	-1.02389	-0.52482	0.43574
O38	-0.98115	-0.43921	0.32933
Cl39	-1.09157	-0.49047	-0.36056
Cl40	-0.91498	-0.56914	-0.01598
H41	-1.09452	-0.55029	0.40875

H42	-0.9101	-0.416	0.35122
H43	-1.12111	-0.52442	-0.08215
H44	-1.0179	-0.46366	-0.29511
H45	-0.98806	-0.46855	-0.06532
H46	-1.01576	-0.55024	0.04811
H47	-0.98658	-0.58361	-0.04463
H48	-0.88556	-0.50304	0.13806
N49	2.24135	0.62304	1.21892
C50	2.25945	0.62192	1.1078
C51	0.7402	0.3791	0.33029
N52	0.75565	0.37597	0.21355
O53	1.28962	0.69063	0.0948
O54	0.71436	0.31435	0.34009
H55	-1.21266	-0.56514	0.03476
H56	-1.14791	-0.52	0.02655
H57	-1.12835	-0.57985	0.37405
H58	-1.19387	-0.62413	0.38151
H59	-0.86162	-0.46622	0.42993
H60	-0.87297	-0.41374	0.03103
H61	-0.80596	-0.37397	0.02261
H62	-0.79447	-0.427	0.41068
H63	2.24567	0.60243	1.01375
H64	0.75651	0.39801	0.4226
H65	-1.03361	-0.51847	0.53815
H66	-0.9622	-0.41436	0.38584
H67	2.25502	0.64012	1.31559
H68	0.74035	0.3549	0.13151

Table S2. The structure model of (*S*)-**BHTP-COF** with *R3* mode.

(*S*)-**BHTP-COF** Space group: *R3* *a* = 43.8379 Å, *b* = 43.8379 Å, *c* = 9.0257 Å *α* = 90.0°, *β* = 90°, *γ* = 120.0°			
Atom	x	y	z
C1	-1.30833	0.32246	0.34009
C2	-1.29726	-0.64152	0.33956
C3	-1.20655	-0.59797	0.20363
C4	-1.1937	-0.56897	0.10834

C5	-1.15759	-0.54413	0.10086
C6	-1.13392	-0.55002	0.18775
C7	-1.14714	-0.57748	0.29382
C8	-1.18337	-0.60149	0.29864
C9	-0.84913	-0.44516	0.34037
C10	-0.87084	-0.44019	0.23735
C11	-0.85548	-0.41581	0.11924
C12	-0.81877	-0.3946	0.11358
C13	-0.79732	-0.39822	0.218
C14	-0.81242	-0.42372	0.32881
C15	-0.70329	-0.35581	0.09487
C16	-0.68907	-0.31924	0.0948
N17	2.24135	0.62304	1.21892
C18	2.25945	0.62192	1.1078
C19	0.7402	0.3791	0.33029
N20	0.75565	0.37597	0.21355
O21	1.28962	0.69063	0.0948
O22	0.71436	0.31435	0.34009
H23	-1.21266	-0.56514	0.03476
H24	-1.14791	-0.52	0.02655
H25	-1.12835	-0.57985	0.37405
H26	-1.19387	-0.62413	0.38151
H27	-0.86162	-0.46622	0.42993
H28	-0.87297	-0.41374	0.03103
H29	-0.80596	-0.37397	0.02261
H30	-0.79447	-0.427	0.41068
H31	2.24567	0.60243	1.01375
H32	0.75651	0.39801	0.4226
C33	0.53867	0.44177	0.17415
C34	0.52076	0.4452	0.04976
C35	0.50591	0.46756	0.0589
C36	0.51035	0.48709	0.19019
C37	0.53065	0.48555	0.30668
C38	0.5442	0.46289	0.29919
C39	0.49327	0.5087	0.21013
C40	0.50773	0.54137	0.1383
C41	0.49129	0.5615	0.1481

C42	0.46041	0.54986	0.23105
C43	0.44685	0.51815	0.31358
C44	0.46299	0.49705	0.30058
C45	0.51782	0.42738	-0.08435
C46	0.49991	0.4308	-0.2054
C47	0.48433	0.45172	-0.19461
C48	0.48702	0.4698	-0.06356
C49	0.44835	0.46477	0.37832
C50	0.41923	0.4542	0.47042
C51	0.40421	0.47543	0.48746
C52	0.41788	0.5072	0.41047
O53	0.53595	0.50498	0.43271
O54	0.53737	0.55325	0.05284
Cl55	0.49722	0.40889	-0.37173
Cl56	0.36819	0.46214	0.60706
H57	0.56003	0.46166	0.39689
H58	0.50296	0.58786	0.0881
H59	0.53014	0.40992	-0.09484
H60	0.46934	0.45409	-0.29301
H61	0.47379	0.48648	-0.05583
H62	0.46036	0.44708	0.36607
H63	0.40762	0.42806	0.53218
H64	0.40541	0.5244	0.42643
H65	2.25502	0.64012	1.31559
H66	0.74035	0.3549	0.13151
H67	0.51013	0.49913	0.47908
H68	0.55895	0.57793	0.10112

Table S3. Comparison of separation performance of three racemic drugs by HPLC columns packed with (*R*)-**BHTP-COF**, and several commercial CSPs.

Chiral drugs	This work		Chiralcel OD-H [9]		Chiralpak AD-H [10]	
	α	Rs	α	Rs	α	Rs
Ibuprofen	2.32	3.39	1.85	1.32	C.S.	C.S.

| Mandelic acid | 2.05 | 3.17 | C.S. | C.S. | 1.08 | 2.39 |
| Naproxen | 2.16 | 2.04 | 2.09 | 2.74 | 2.28 | 4.45 |

C.S.: Cannot be seperated.

Table S4. Enantioseparation data on the (*S*)-**BHTP-COF** packed HPLC column.

Chiral drugs	α	Rs	Mobile phase
Ibuprofen	2.18	3.20	a
Mandelic acid	1.94	3.11	a
Ketoprofen	1.52	3.63	a
Naproxen	2.09	2.16	b
Propranolol	1.77	2.15	c
Cetirizine	2.69	2.74	c

7. References

[1]   C. Valente, E. Choi, M. E. Belowich, C. J. Doonan, Q. Li, T. B. Gasa, Y. Y. Botros, O. M. Yaghi, J. F. Stoddart, *Chem. Commun.*, 2010, **46**, 4911-4913.

[2] M. J. Frisch, G. W. Trucks, H. B. Schlegel, G. E. Scuseria, M. A. Robb, J. R. Cheeseman, G. Scalmani, V. Barone, G. A. Petersson, H. Nakatsuji, X. Li, M. Caricato, A. V. Marenich, J. Bloino, B. G. Janesko, R. Gomperts, B. Mennucci, H. P. Hratchian, J. V. Ortiz, A. F. Izmaylov, J. L. Sonnenberg, D. Williams-Young, F. Ding, F. Lipparini, F. Egidi, J. Goings, B. Peng, A. Petrone, T. Henderson, D. Ranasinghe, V. G. Zakrzewski, J. Gao, N. Rega, G. Zheng, W. Liang, M. Hada, M. Ehara, K. Toyota, R. Fukuda, J. Hasegawa, M. Ishida, T. Nakajima, Y. Honda, O. Kitao, H. Nakai, T. Vreven, K. Throssell, J. A. Montgomery, Jr., J. E. Peralta, F. Ogliaro, M. J. Bearpark, J. J. Heyd, E. N. Brothers, K. N. Kudin, V. N. Staroverov, T. A. Keith, R. Kobayashi, J. Normand, K. Raghavachari, A. P. Rendell, J. C. Burant, S. S. Iyengar, J. Tomasi, M. Cossi, J. M. Millam, M. Klene, C.

Adamo, R. Cammi, J. W. Ochterski, R. L. Martin, K. Morokuma, O. Farkas, J. B. Foresman, and D. J. Fox,

Gaussian 16, Revision A.03, Gaussian, Inc., Wallingford CT, 2016.

[3] A. D. Becke, J. *Chem. Phys.*, 1993, **98**, 5648–5652.

[4] C. Lee, W. Yang, R. G. Parr, *Phys. Rev. B: Condens. Matter Mater. Phys.*, 1988, **37**, 785–789.

[5] S. Grimme, J. Antony, S. Ehrlich, H. Krieg, *J. Chem. Phys.*, 2010, **132**, 154104.

[6] F. Weigend, R. Ahlrichs, *Phys. Chem. Chem. Phys.*, 2005, **7**, 3297−3305.

[7] F. Weigend, *Phys. Chem. Chem. Phys.*, 2006, **8**, 1057−1065.

[8] C. Y. Legault, CYLview, 1.0b, Université de Sherbrooke, 2009, http://www.cylview.org.

[9] H. Y. Aboul-Enein, L. I. Abou-Basha, S. A. Bakr, *Chirality*, 1996, **8**, 153–156.

[10] O. Yoshio, A. Ryo, F. Tohru, H. Koichi, *Chem. Lett.*, 1987, **16**, 1857–1860.